ISSN (Print) : 0974-6846
ISSN (Online) : 0974-5645
Indian Journal of Science and Technology, *Vol 8(S8), 493-503, April 2015* DOI: 10.17485/ijst/2015/v8iS8/70748

Design of Fuzzy Logic Controller for Inverted Pendulum-type Mobile Robot using Smart In-Wheel Motor

Kwak Sangfeel[1], Song Eunji[1], Kim KyungSik[2] and Song ByungSeop[2*]

[1]Rovitek Co
[2]Department of Rehabilitation, Science & Technology, Daegu University, 201, Daegudae-ro, Gyeongsan, Gyeongsangbuk-do Province, Korea; bssong@daegu.ac.kr

Abstract

Some researches for inverted pendulum-type mobile robots have been presented in many articles. In this paper we present the design of a fuzzy logic controller (FLC) for an inverted pendulum-type mobile robot. Its mathematical model is firstly analyzed, and then we get its parameters through some manipulations. The FLC is good for some nonlinear plants. We design a conventional FLC for inverted pendulum-type mobile robot and show some simulation results.

Keywords: Inverted Pendulum, Mobile Robot, Fuzzy Logic Controller (FLC)

1. Introduction

Many researchers have recently studied inverted pendulum-type mobile robot including development of inverted pendulum-type mobile two-wheeled vehicle at home and abroad[1]. The inverted pendulum-type two-wheeled vehicleis a system that added mobility by using dynamic function to balance the inverted pendulum[1]. The balancing system is similar to the controlling mechanism for a biped robot modeled after a person keeping balance with two feet while moving[3]. The inverted pendulum system has been frequently used as a control model for controller verification in many studies that covered the theory on non-linear controller[4]. The study designed a fuzzy logic controller for non-linear dynamics model of the inverted pendulum-type mobile robot and verified its function through simulation.

2. Design & Analysis

The inverted pendulum-type mobile robot consists of two wheels and a pole in between. The system measures tilting of this pole using tilting sensor, acceleration and gyro sensor and maintains the tilted angle at 0°. This system is generally called ZMP (Zero Moment Point) control system[2].

2.1 Dynamics Model for the Inverted Pendulum-Type Mobile Robot

Designing the controller first needs motion equation of the inverted pendulum-type mobile robotand identification of system model. The following is physical parameters of the inverted pendulum-type mobile robot.

x : robotdisplacement (m)
M_W : wheel weight (kg)
J_W : wheel moment of inertia ($kg \cdot m^2$)
r : wheel radius (m)
l: pole length (m)
M_p : weight for the pole's center of gravity (kg)
J_p : moment of inertia for the pole's center of gravity ($kg \cdot m^2$)

*Author for correspondence

g: gravity acceleration (m/s^2)
θ: tilted angle of the pole (rad)
ϕ: rotation angle of wheel (rad)
V: reaction force of pole for vertical direction
H : reaction force of pole for horizontal direction
H_W : reaction force of wheel for horizontal direction
f_W: unknown input for wheel
f_p: unknown input for pole
τ: wheel torque
x_p: pole displacement foraxis$x$
y_p: pole displacement foraxis y

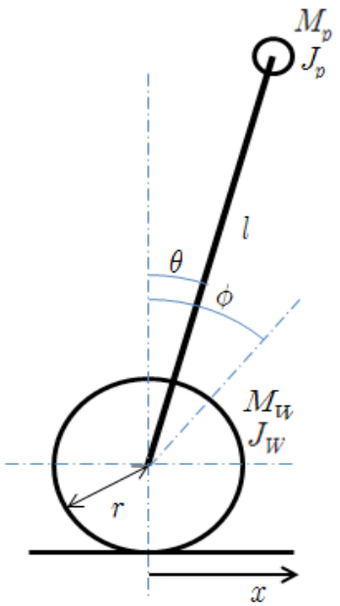

Figure 1. Dynamics model of the inverted pendulum-type mobile robot.

2.1.1 Wheel dynamics equation

The inverted pendulum-type mobile robot can be divided into two parts: wheelsand motor and body pole that supports the body and keeps balance with the wheels. The model can be described with sum of the wheel dynamics equation for the drive shaft, reaction force of the pole's vertical and horizontal axis and wheel moment of inertia.

$$M_W \ddot{x} = H + f_W + H_W \quad (1)$$

$$J_W \ddot{\phi} = -rH_W + \tau \quad (2)$$

Equation (1) and (2) showed the relation between wheel moment of inertia and reaction force from the pole.

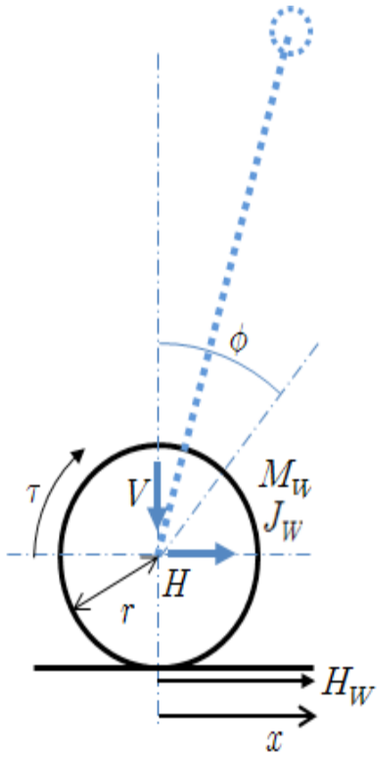

Figure 3. Wheel dynamics.

Robot displacement x and wheel rotation angle ϕ had the following relation:

$$r\ddot{\phi} = \ddot{x} \quad (3\text{-}1)$$

$$\ddot{\phi} = \frac{\ddot{x}}{r} \quad (3\text{-}2)$$

When Equation (2) and (3)were combined, H_W could be described as the following equation for τ and x :

$$H_W = \frac{\tau}{r} - \frac{J_W}{r^2}\ddot{x} \quad (4)$$

The following was Equation (1) combined with Equation (4):

$$\left(M_W + \frac{J_W}{r^2}\right)\ddot{x} = H + f_W + \frac{\tau}{r} \quad (5)$$

2.1.2 Pole dynamics equation

The illustration below showed the force given to the body that consisted of the motor and pole except for the wheels.

Displacement of the pole's center of gravity for horizontal direction was:

$$x_p = x + l\sin\theta \quad (6)$$

When Equation (6) went through two sets of differential for time, it could be shown as:

$$\ddot{x}_p = \ddot{x} + l\ddot{\theta}\cos\theta - l\dot{\theta}^2\sin\theta \quad (7)$$

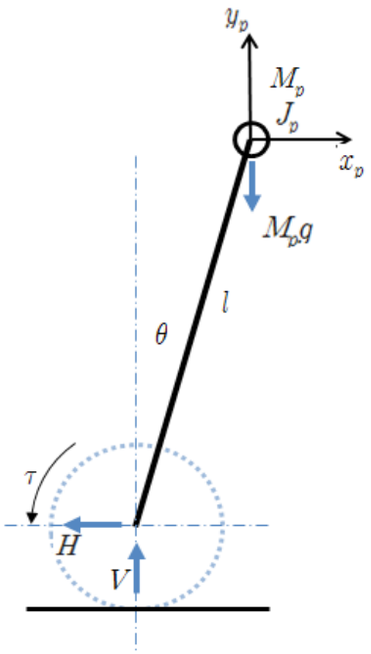

Figure 3. Pole dynamics.

Equation (7) could be described as dynamics equation for axis x for the pole's center of gravity as:

$$M_p\ddot{x}_p = f_p - H \quad (8)$$

$$H = -(M_p\ddot{x} + M_p l(\ddot{\theta}\cos\theta - \dot{\theta}^2\sin\theta)) + f_p \quad (9)$$

y_p, which was pole displacement foraxis y could be described as:

$$y_p = l\cos\theta \quad (10)$$

Two sets of differentials for time for Equation (10) brought about:

$$\ddot{y}_p = -l(\dot{\theta}^2\cos\theta + \ddot{\theta}\sin\theta) \quad (11)$$

With Equation (11), the dynamics equation for axis y for pole's center of gravity could be:

$$M_p\ddot{y}_p = V - M_pg \quad (12)$$

$$V = -M_p l(\dot{\theta}^2\cos\theta + \ddot{\theta}\sin\theta) + M_pg \quad (13)$$

Equation (9) and (5) could be presented as:

$$\left(M_W + M_p + \frac{J_W}{r^2}\right)\ddot{x} + M_p l\cos\theta\ddot{\theta} - M_p l\sin\theta\dot{\theta}^2 = f_W + f_p + \frac{1}{r}\tau \quad (14)$$

Where, acceleration was $\ddot{x}$, angular acceleration was $\ddot{\theta}$ and torque was τ.

Moment of inertia for the pole's center of gravity was:

$$J_p\ddot{\theta} = Vl\sin\theta - Hl\cos\theta - \tau \quad (15)$$

Combining Equation (9) and (13) showed:

$$(J_p + M_p l^2)\ddot{\theta} + M_p l\ddot{x}\cos\theta - M_p gl\sin\theta = l\cos\theta f_p - \tau \quad (16)$$

Where angular acceleration was $\ddot{\theta}$, acceleration was $\ddot{x}$ and torque was τ.

3. State Equation of Linear Model

When it was assumed that tilted angle of the pole θ was very small,

$$\sin\theta \approx \theta \quad (17)$$

$$\cos\theta = 1 \quad (18)$$

it could be approximated like Equation (17) and (18) and approximated to $\dot{\theta}^2 = 0$.

$$\left(M_W + M_p + \frac{J_W}{r^2}\right)\ddot{x} + M_p l\ddot{\theta} = f_W + f_p + \frac{1}{r}\tau \quad (19)$$

$$(J_p + M_p l^2)\ddot{\theta} + M_p l\ddot{x} - M_p gl\theta = lf_p - \tau \quad (20)$$

To establish state equation, Equation (19) and (20) could be changed to the equation about $\ddot{x}$ and $\ddot{\theta}$ as below:

$$\begin{vmatrix}\ddot{x}\\ \ddot{\theta}\end{vmatrix} = \begin{vmatrix}A_{11}\\ A_{12}\end{vmatrix} \quad (21)$$

When it was put as unknown inputs at Equation (21)

$$f_W = f_p = 0 \quad (22),$$

Equation (23) was produced like:

$$\begin{vmatrix}\ddot{x}\\ \ddot{\theta}\end{vmatrix} = \begin{vmatrix}A_{11}'\\ A_{12}'\end{vmatrix} \quad (23)$$

It could be expressed as state equation based on Equation (23):

$$x_s = (x_1\ \ x_2\ \ x_3\ \ x_4)^T,$$

$$x_1 = x,\ \ x_2 = \dot{x},\ \ x_3 = \theta,\ \ x_4 = \dot{\theta} \quad (24)$$

$$\dot{x}_s = Ax_s + Br \quad (25)$$

$$\dot{x}_1 = \dot{x} = x_2$$

$$\dot{x}_2 = A_1'$$

$$\dot{x}_3 = \dot{\theta} = x_4$$

$$\dot{x}_4 = A_2' \quad (26)$$

4. State Equation of Non-Linear Model

If the constant of Equation (14) and (16)could be put as:

$$W = (M_w + M_p + \frac{J_w}{r^2}) \quad (27)$$

$$P = J_p + M_p l^2 \quad (28)$$

$$Q = M_p l \quad (29)$$

the following could come up:

$$Q\cos\theta\ddot{\theta} + W\ddot{x} - Q\sin\theta\dot{\theta}^2 = \frac{1}{r}\tau \quad (30)$$

$$P\ddot{\theta} + Q\cos\theta\ddot{x} - Q\sin\theta g = -\tau \quad (31)$$

When, Equation (30) and (31) were expressed as those for $\ddot{x}$ and $\ddot{\theta}$,

$$\begin{vmatrix} \ddot{x} \\ \ddot{\theta} \end{vmatrix} = \begin{vmatrix} A_{n1} \\ A_{n2} \end{vmatrix} \quad (32)$$

Equation (32) above was produced.With this, state equation was induced as:

$$\dot{x}_1 = \dot{x} = x_2$$
$$\dot{x}_2 = A_{n1}$$
$$\dot{x}_3 = \dot{\theta} = x_4$$
$$\dot{x}_4 = A_{n2} \quad (33)$$

5. Linear Controller Design and Simulation for Linear Model

The physical parameters of the inverted pendulum-type robot to be simulated for the study were as below4:

M_W: 0.076 (kg)
J_W: 3.42E -5 $(kg \cdot m^2)$
r: 0.03 (m)
l : 0.15 (m)
M_B: 0.6 (kg)
J_B: 1.34E-2 $(kg \cdot m^2)$
g: 9.81 (m/s^2)

The following showed coefficient of each matrix for Equation (25):

$$A = \begin{vmatrix} 0 & 1 & 0 & 0 \\ 0 & 0 & -7.1544 & 0 \\ 0 & 0 & 0 & 1 \\ 0 & 0 & 56.7582 & 0 \end{vmatrix} \quad (34)$$

$$B = \begin{vmatrix} 0 \\ 88.8361 \\ 0 \\ -334.3958 \end{vmatrix} \quad (35)$$

When controllability for the system was distinguished, it became $rank|b\ Ab\ A^2b\ A^3b| = 4$ and n is 4. Therefore, the system had controllability. When arbitrary pole was assumed as (36) to design a controller,

$$P_{co} = |-4\ -3\ -2\ -1| \quad (36)$$

following could be gained:

$$K_{co} = \begin{vmatrix} -0.0091 \\ -0.0189 \\ -0.2768 \\ -0.0349 \end{vmatrix}^T \quad (37)$$

Controller block diagram for Equation (37) could be illustrated as shown:

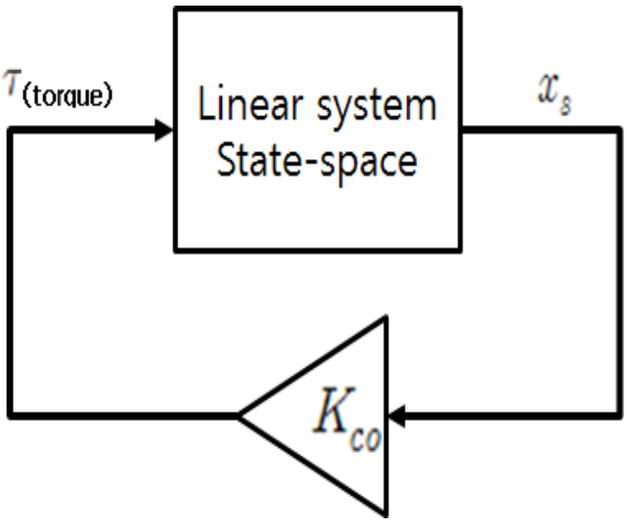

Figure 4. Controller block diagram.

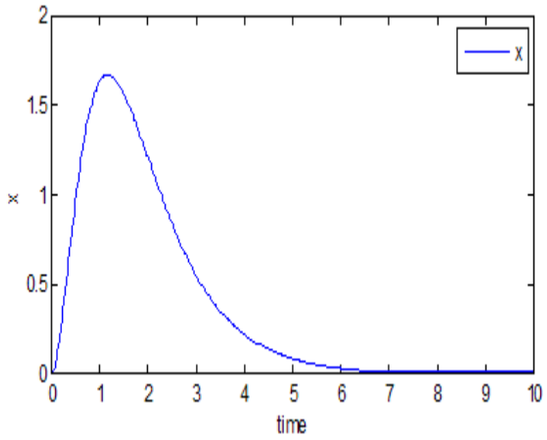

Figure 5. Graph on displacement x_1.

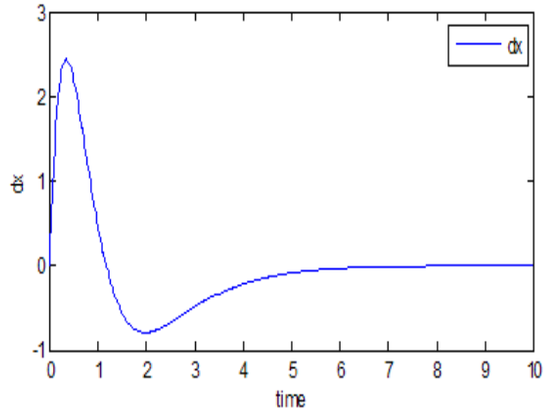

Figure 6. Graph on traveling velocity x_2.

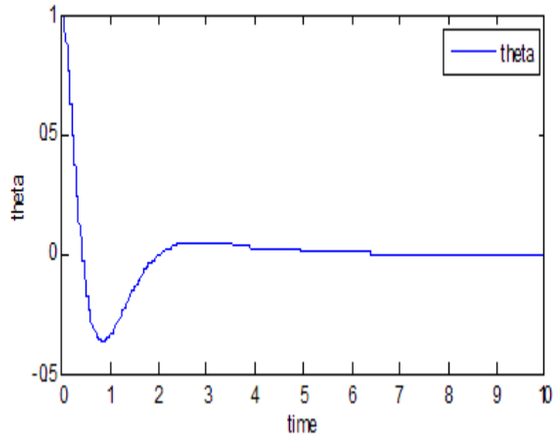

Figure 7. Graph onpole's tilting angle x_3.

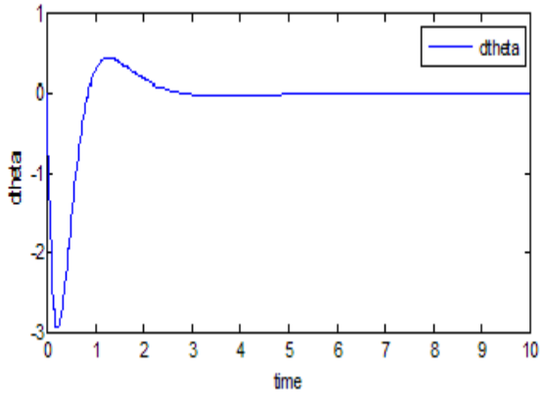

Figure 8. Graph on pole's angular velocity x_4.

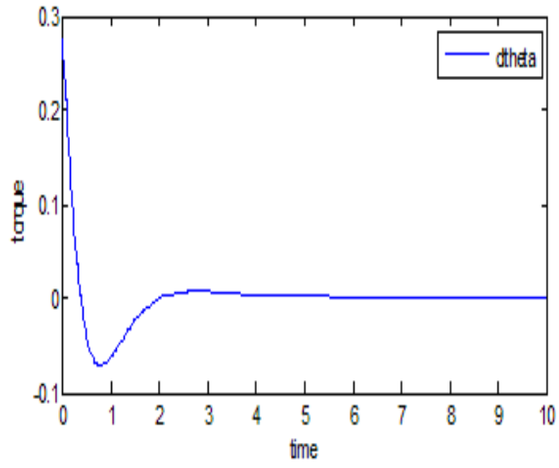

Figure 9. Graph on torque.

The simulation results of the linear controller for the linear system were shown from Figure 5-9 where displacement of the inverted pendulum-type mobile robot was x_1, velocity was x_2, pole's tilting angle was x_3, pole's angular velocity was x_4 and torque. If the initial value of x_3 was put 1, it was found the system stabilized with the control input torque for the controller.

6. Design of Fuzzy Logic Controller for Linear Model

Important parameters that decide stability of the inverted pendulum-type mobile robot were θ and $\dot{\theta}$. With the linear controller, controlling size can be checked as below:

$\theta : -1 \leqq \theta \leqq 1$

$\dot{\theta} : -3 \leqq \theta \leqq 3$

$Torque : -0.5 \leqq Torque \leqq 0.5$

Here, the study could achieve the following when θ value was maintained 0 and feedback controller was structured so that position could be controlled fordisplacement x.

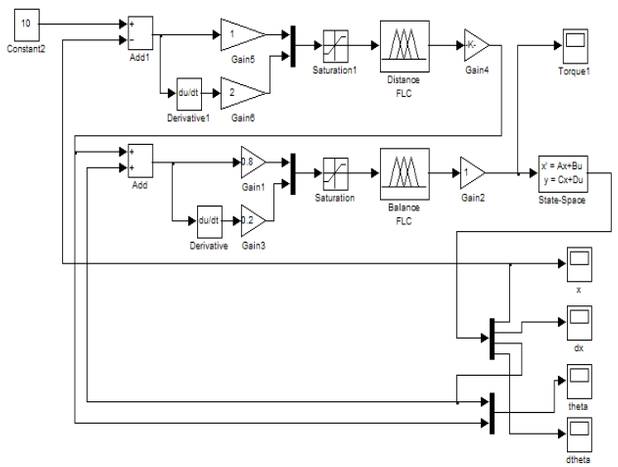

Figure 10. Figure 10. Fuzzy logic controller.

6.1 Fuzzy Membership Function

This controller comprised Distance FLC to control moved position and Balance FLC to balance the pole. Distance FLC input was the error between the current position and set position and the difference while its output was angular weight of the pole error to control the robot's movement. In the meantime, Balance FLC input was the sum of the current pole angle θ and angular weight of the pole error, the output of Distance FLC, and the output was torque to control the motor.

6.1.1 Distance FLC's Membership Function and Inference Rule

The following showed the membership function for the input and output of Distance FLC.

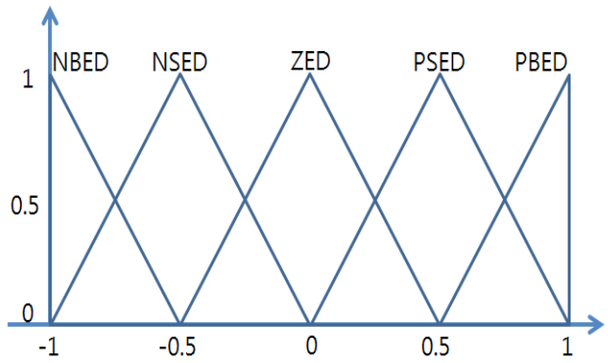

Figure 11. Membership function for input parameter edist.

edist : Distance Error input
NBED : Negative Big Error Distance
NSED : Negative Small Error Distance
ZED : Zero Error Distance
PSED : Positive Small Error Distance
PBED : Positive Big Error Distance

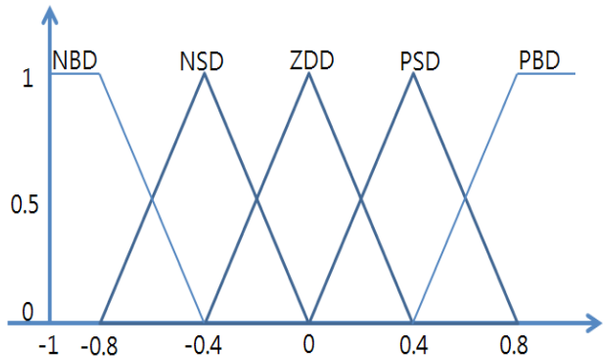

Figure 12. Membership function for input parameter dedist

dedist : Diff Distance Error input
NBD : Negative Big Diff Error Distance
NSD : Negative Small Diff Error Distance
ZDD : Zero Error Diff Error Distance
PSD : Positive Small Diff Error Distance
PBD : Positive Big Diff Error Distance

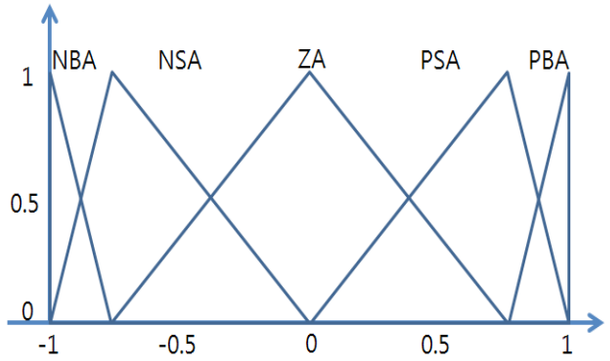

Figure 13. Membership function for output parameter.

AddAngle
AddAngle : Add Angle
NBA : Negative Big Angle
NSA : Negative Small Angle
ZA : Zero Angle
PSA : Positive Small Angle
PBA : Positive Big Angle

Implication: If edist is A and dedist is B then AddAngle is C

Table 1. Rule table for distance FLC

ed \ ed'	NBD	NSD	ZDD	PSD	PBD
NBED	PBA	PBA	PBA	PSA	ZA
NSED	PBA	PBA	PSA	ZA	NSA
ZED	PBA	PSA	ZA	NSA	NBA
PSED	PSA	ZA	NSA	NBA	NBA
PBED	ZA	NSA	NBA	NBA	NBA

6.1.2 Balance FLC's Membership Function and Inference Rule

The following presented the membership function for the input and output of Balance FLC.

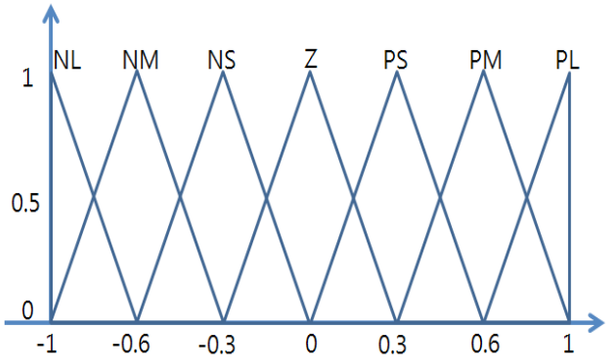

Figure 14. Membership function for input parameter etheta.

etheta : Error Angle Theta
NL : Negative Large
NM : Negative Medium
NS : Negative Small
Z : Zero
PS : Positive Small
PM : Positive Medium

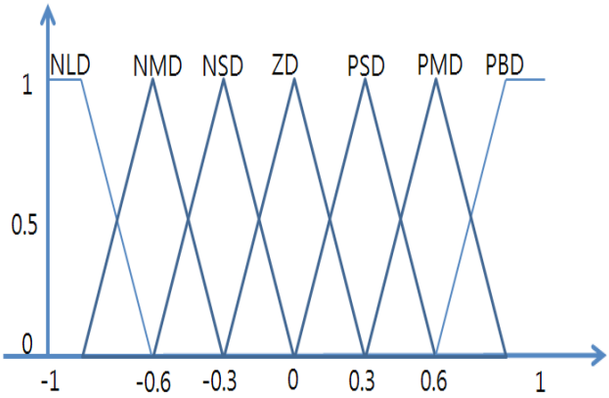

Figure 15. Membership function for input parameter detheta.

detheta : Diff Error Angle Theta
NLD : Negative Large Diff Error
NMD : Negative Medium Diff Error
NSD : Negative Small Diff Error
ZD : Zero Diff Error
PSD : Positive Small Diff Error
PMD : Positive Medium Diff Error
PLD : Positive Large Diff Error

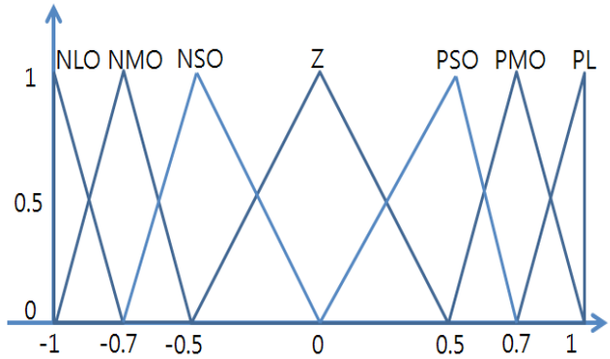

Figure 16. Membership function for output parameter torque.

Torque : Torque Output
NLO : Negative Large Output
NMO : Negative Medium Output
NSO : Negative Small Output
ZO : Zero Output
PSO : Positive Small Output
PMO : Positive Medium Output
PLO : Positive Large Output

ZO Membership of torque output was wide open and it became narrower towards NLO and PLO. With this form, vibration of the output was reduced and normal condition was kept stably.

Implication : If etheta is A and detheta is B then Torque is C

Table 2. Rule table for balance FLC

e \ e'	NLD	NMD	NSD	ZD	PSD	PMD	PLD
NL	NLO	NLO	NLO	NMO	NMO	NMO	NSO
NM	NLO	NLO	NMO	NMO	NSO	NSO	PSO
NS	NLO	NMO	NSO	NSO	ZO	PSO	PSO
Z	NMO	NSO	NSO	ZO	PSO	PSO	PMO
PS	NSO	NSO	ZO	PSO	PSO	PMO	PLO
PM	NSO	PSO	PSO	PMO	PMO	PLO	PLO
PL	PSO	PMO	PMO	PMO	PLO	PLO	PLO

In composing the two FLCs, AND computation had minimum value, OR computation had maximum value and inference used Mamdani method.Defuzzification used center of gravity method to obtain sensible results.

6.1.3 Simulation Result of FLC for Linear Model

The simulation result could be expressed as the following figures with AddAngle, torque, displacement x, velocity $\dot{x}$, pole's tilting angle θ, pole's angular velocity $\dot{\theta}$. As the initial condition of the robot, the pole tilted 1 radian positive and the target distance was set at 10m for simulation.

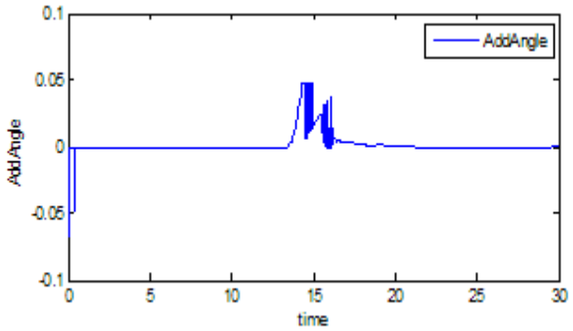

Figure 17. Graph on AddAngle.

For the 10m given above, AddAngle of Distance FLC output was authorized as Balance FLC input. The above graph showed AddAngle output.

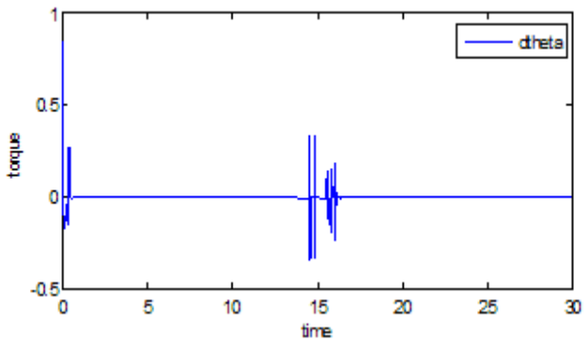

Figure 18. Graph on torque.

Figure 18 was Balance FLC output, which was the motor torque input for the inverted pendulum-type mobile robot linear model. Torque was authorized for initial movement and kept as fine value. When it reached target position, it was found that the robot pole's angle was stabilized and torque was generated to halt.

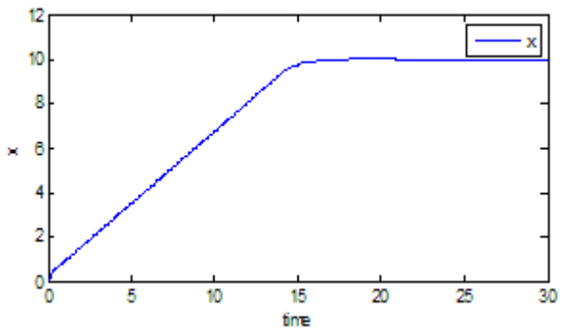

Figure 19. Graph on displacement x_1.

Figure 19 showed displacement. The robot stopped after reaching the target position by traveling 10m.

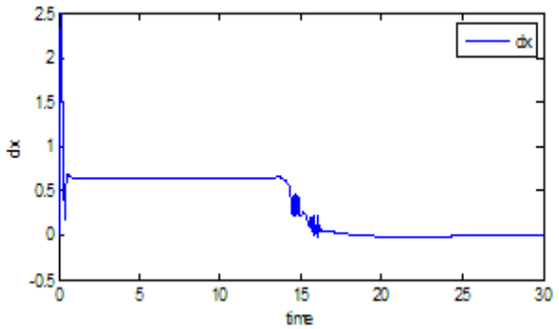

Figure 20. Graph on traveling velocity.

Figure 20 displayed the robot's velocity of about 0.7m/s before it stopped.

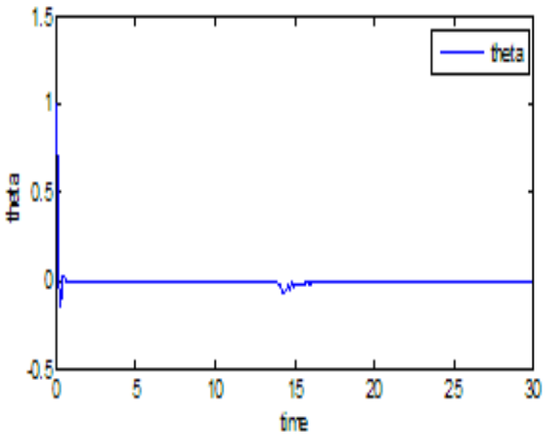

Figure 21. Graph on pole's tilting angle.

Figure 21 presented the pole's tilting angle with the robot's movement. It was found the robot moved while maintaining balance of the pole. When the weight graph of AddAngle was compared, AddAngle and tilting angle reacted against each other during acceleration and deceleration of the robot.

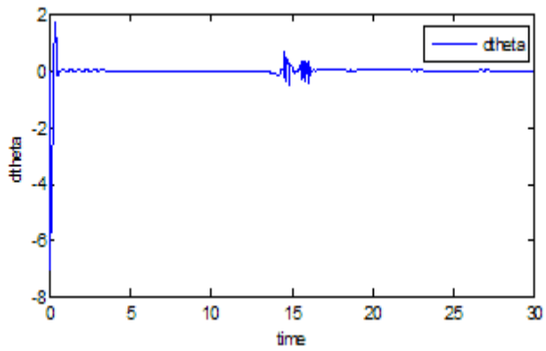

Figure 22. Graph on pole's angular velocity.

Figure 22 covered the pole's angular velocity.

6.1.4 Simulation Result for Non-Linear Model

Leaving the controller composition as it was, the study changed the state equation of the control system from linear to non-linear model to execute simulation.

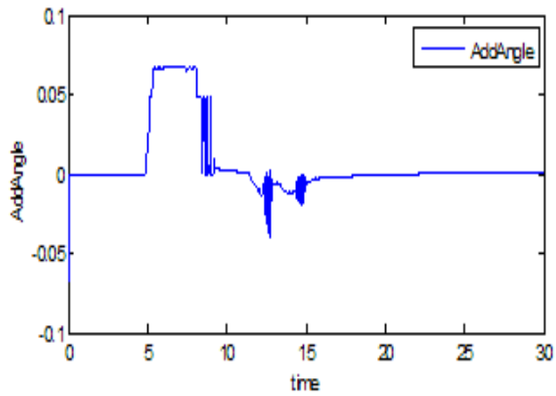

Figure 23. Graph on AddAngle for non-linear model.

Figure 23 showed changing Distance FLC output AddAngle. The robot began to move using the initial pole tilting and reaction force from the moment it reached its target position caused AddAngle to stop it with controlling power.

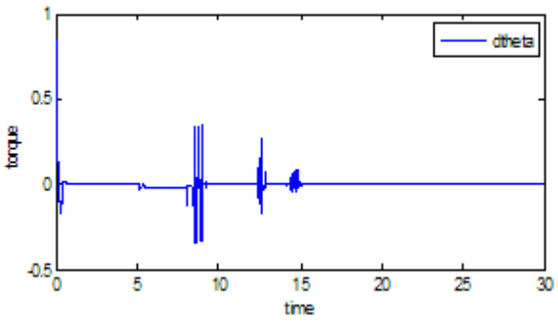

Figure 24. Graph on torque for non-linear model.

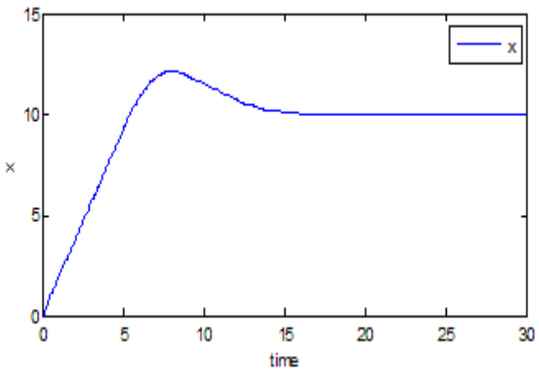

Figure 25. Graph on displacement x_1 for non-linear model.

Figure 24 showed motor torque to operate the inverted pendulum-type mobile robot. Big torque was generated for initial robot acceleration and fine torque was maintained when it was in motion. When it reached its target position, torque was generated for reverse acceleration from the moment overshoot occurred.

Figure 25 showed the robot displacement and Figure 26 showing its changing movement velocity.

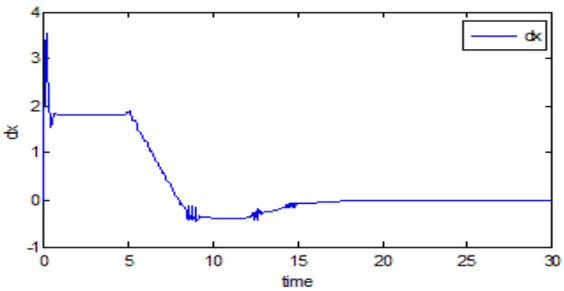

Figure 26. Graph on robot velocity x_2 for non-linear model.

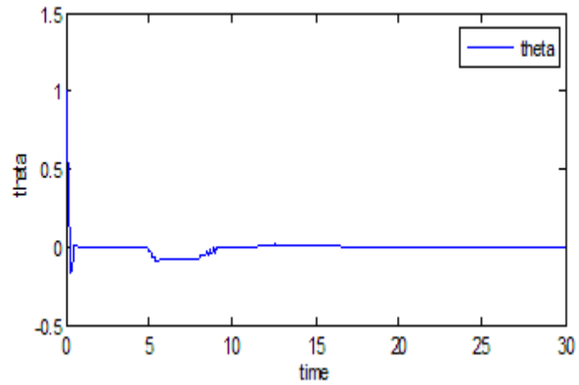

Figure 27. Graph on pole angle x_3 for non-linear model.

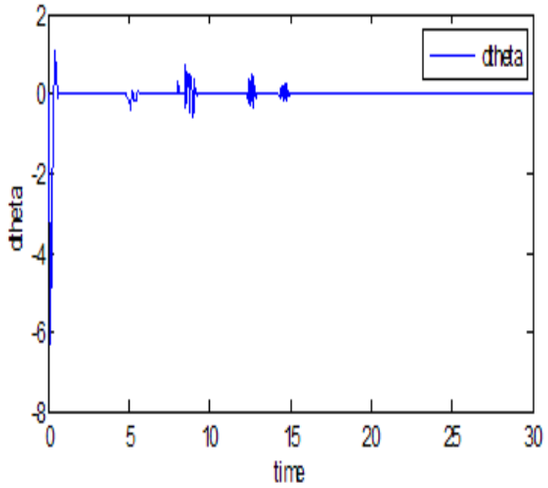

Figure 27. Graph on pole angular velocity x_4 for non-linear model.

As Figure 26 and Figure 27 showed, the displacement converged toward the 10m target position. It was also found the robot pole balance also converged toward 0 except for the change of reaction force size occurring when the robot accelerated or decelerated.

7. Smart In-Wheel Motor

Smart In-Wheel Motor refers to the motor that contains motor, decelerator, motor driver, controller, encoder and current sensor inside the wheel. This type is appropriate for the driving system like a robot as the structure is simple. The study applied 200W Smart In-Wheel motor.

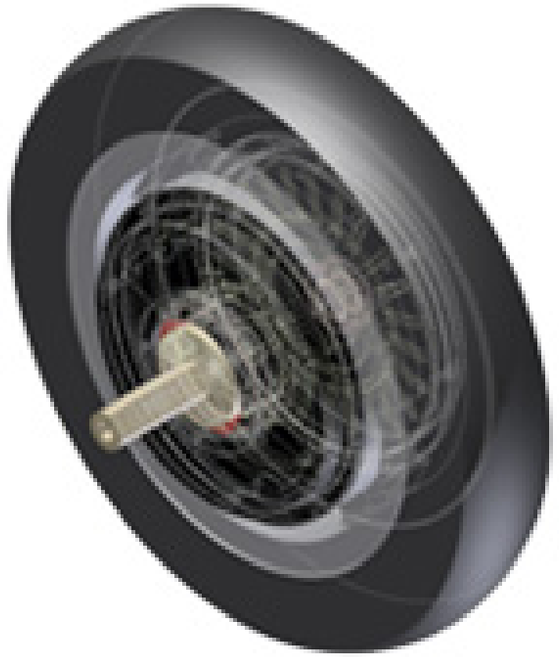

Figure 30. Smart in-wheel motor.

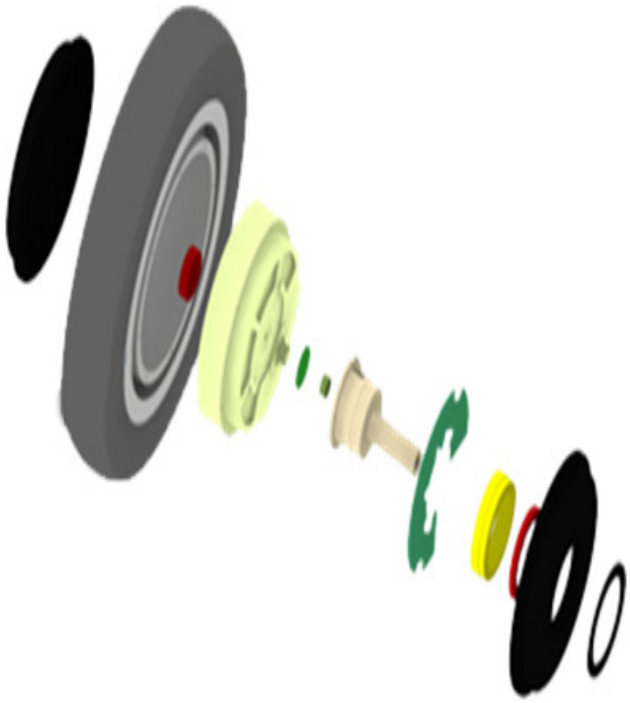

Figure 31. Structure of smart in-wheel motor.

8. Conclusion

The study confirmed the dynamics model of the non-linear inverted pendulum-type mobile robot, induced the linear controller using linear model to structure non-linear controller for it and performed simulation, allowing obtaining approximate size for the input and output. It also designed Distance FLC that controlled traveling distance based on the scope of the acquired input and output as well as Balance FLC that maintained balance of the pole angle and controlled the linear and non-linear model respectively through simulation. It was found from the study that complex non-linear system could be appropriately controlled with a relatively simple FLC design. Following this, it will reduce the amount of calculation with modified design of a simple structured FLC through further study on its control feature and construct the system as the embedded system based on this. With the embedded system, the improved FLC controller will be operated to verify performance.

9. Acknowledgement

This work (Grants No. C0238638) was supported by Business for Academic-industrial Cooperative establishments funded Korea Small and Medium Business Administration in 2014.

10. References

1. Segway. Available from: http://www.segway.com
2. Park JH. Fuzzy-logic zero-moment-point trajectory generation for reduced trunk motion of biped robots. Fuzzy Set Techniques for Intelligent Robotic Systems. 2003 Feb 16; 134(1):189–203.
3. Yoon JH, Park JH. Locomotion control of biped robots with serially-linked parallel legs. Transaction of the Korean Soc, Mech. Eng A. 2010; 34(6):683–93.
4. Lee SH, RheeSY. Dynamic modeling of a wheeled inverted pendulum forinclined road and changing its center of gravity. Korean Institute of Intelligent Systems. 2012; 22(1):69–74.
5. Lee SH, Park JK. Simulation for implementing attitude controller of wheeled inverted pendulum. The Korean Society of Mechanical Engineers Gyungnam Region 2006 Conference; 2006; p.191–96.
6. Ha HU, Lee JM. A control of mobile inverted pendulum using single accelerometer. Institute of Control Robotics and Systems. 2010; 16(5):2012.5
7. Nawawi SW, Ahmad MN, Osman JHS. Controll of two-wheels inverted Pendlum Mobile Robot using full order sliding mode control. Proceedings of International Conference on Man-Mahcine System 2006. Sept 15-16. 2006; Lankawi, Malaysia.
8. Axelsson P, JungY. Lego segway project report. Technical report from automatic control at linkopings universitet. Devision of Automatic Control; 2011.